Dynamical scenarios of mutually delay-coupled semiconductor lasers in the short coupling regime

Eric Wille, Michael Peil, Ingo Fischer and Wolfgang Elsäßer

Darmstadt University of Technology, Institute of Applied Physics,
Schloßgartenstraße 7, D-64289 Darmstadt, Germany

ABSTRACT

We present experimental and numerical studies of the dynamics of two delay-coupled device-identical semiconductor lasers. We concentrate on the regime of short delay times where the coupling delay is comparable to the period of the relaxation oscillation frequency. We find characteristic scenarios in the intensity dynamics depending on the spectral detuning and the coupling phase. For small spectral detuning, the coupled lasers lock to the same frequency and exhibit stable emission. For larger detuning, we find pronounced oscillations of the output intensity. The frequency of oscillation shows a stair-like behavior which depends on the detuning frequency, the coupling time and the coupling phase. In addition, the coupling phase also affects the oscillation frequency and the phase relation between the two oscillating lasers.

Keywords: semiconductor lasers, delay systems, nonlinear dynamics, coupled oscillators

1. INTRODUCTION

Studies on the dynamical behavior of delay-coupled semiconductor lasers (SL) are of current interest for fundamental research and technical applications. For fundamental research, SL are an excellent model system for investigating the properties of delay-coupled oscillators that occur in many systems like neural networks, chemical reactor systems or electronic circuits.[1–3] The influence of a time delay in the coupling becomes important if the delay introduced for example by the spatial distance of the individual oscillators is comparable or larger than the characteristic frequencies of the oscillators. The consequence of such a delay can be a crucial change in the dynamics of the coupled system. Two of the recently studied phenomena induced by a delay are amplitude death[4] and symmetry breaking.[5] A further motivation to study delay-coupled SL is their potential to contribute to new photonic applications. Since SL are the basis for optical communication, their dynamical behavior is of high importance for advancing the technology in this field. Unidirectionally coupled SL can be used for secure data transmission using chaotic carrier signals.[6,7] Furthermore, self-pulsating bidirectionally coupled SL can be applied for optical clock recovery.[8]

These fundamental questions and new applications can be studied experimentally with great precision as SL can be manufactured with well defined parameters and laboratory experiments under stable conditions can be carried out. Furthermore, the nonlinear dynamics of a single semiconductor laser is well studied and numerical models can be used to compare experiment and theory.

In this article, we present experimental and numerical results for a system of two device-identical delay-coupled single mode SL. So far, previous studies mainly concentrated on long delay times, where the coupling time is much larger than the relaxation oscillation period of the lasers.[9,10] In this long coupling time regime, dynamical phenomena such as low frequency fluctuations, chaos synchronization and symmetry breaking have been reported.[9,11] We present studies concentrating on short delay times comparable to the relaxation oscillation period of the lasers in order to give new insight into the understanding of delay-coupled SL. In this context, we concentrate on the influence of spectral detuning between the two SL and the coupling phase. Theoretical analysis of the bifurcation properties depending on these two parameters can be found in the references[12,13] for a model system based on rate equations. This article is organized as follows. The experimental setup and

Further author information: (Send correspondence to E. Wille or I. Fischer)
E. Wille: E-mail: eric.wille@physik.tu-darmstadt.de
I. Fischer: E-mail: ingo.fischer@physik.tu-darmstadt.de

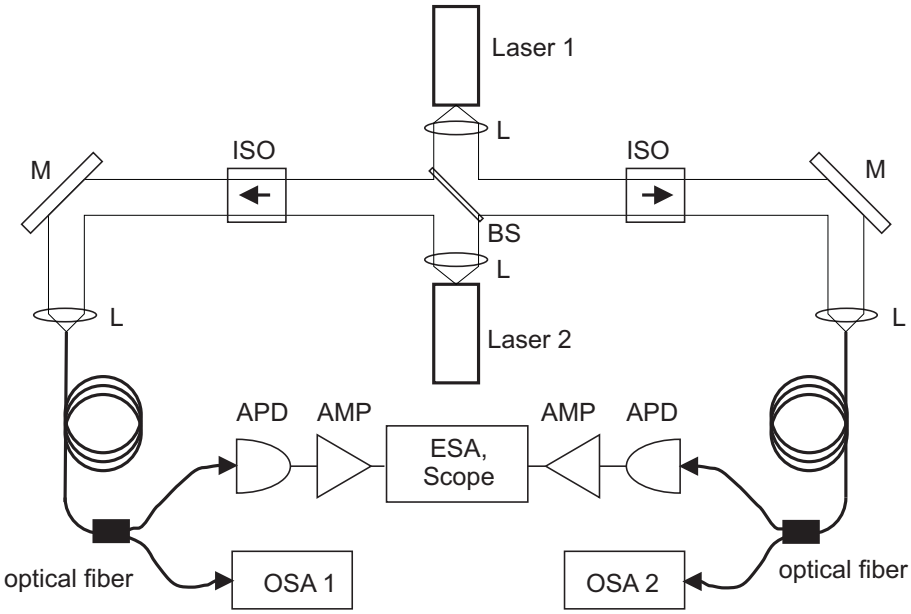

Figure 1. Scheme of the experimental setup. The lasers are coupled via mutual injection of the emitted light by two lenses (L). A part of the light is extracted by the beamsplitter (BS) and analyzed in the detection branches, which are separated by optical isolators (ISO). Furthermore, APD denotes the avalanche photodiodes, AMP rf-amplifiers, ESA the electrical spectrum analyzer, OSA optical spectrum analyzers and M mirrors.

the laser structures are described in section 2. In section 3 we present the different dynamical regimes that occur depending on the spectral detuning. Subsequently, we discuss the influence of the coupling phase on the dynamical regimes in section 4. The rate equation model and the numerical results are presented in section 5. Finally, we summarize the conclusions from our results in section 6.

2. EXPERIMENTAL SETUP

Fig. 1 depicts a scheme of the experimental setup. The output of each laser is collimated by a lens (L), propagates along the coupling distance and is refocused into the active region of the opposite laser. Hence, the two SL are coupled via their lasing electromagnetic field that is dominated by the TE-mode due to the polarization selective laser resonators.

We use two device-identical 1540 nm single mode InGaAsP DFB lasers which had been grown on the same wafer in order to achieve well-matched parameters. The optical spectra agree within 0.05 nm, the threshold current (9.3 mA) within 1% and the relaxation oscillation frequency within 5%. The linewidth broadening factor has been determined to be approximately $\alpha = 2$. The temperature of the lasers is controlled with an accuracy better than 0.01 K. An optical detuning Δf between the lasers can be realized by varying the temperature of one laser, resulting in a shift of the emission frequency of -12.1 GHz/K. Both lasers are pumped at 60 mA with a low-noise dc current source. Under these conditions the relaxation oscillation frequency has been extrapolated to be about 15 GHz.

A beamsplitter (BS) is placed between the lasers which couples out half of the emission power of each laser which is used for analysis of the optical and the dynamical properties in the detection branches (see Fig. 1). The detection branches are separated from the lasers by two optical isolators (ISO) in order to prevent unwanted feedback. The light is coupled into optical single mode fibers and distributed to the measurement devices. The optical spectra are measured using two optical spectrum analyzers (OSA) with a resolution of better than 0.05 nm. The intensity dynamics are analyzed with two fast avalanche photodiodes (APD) with a bandwidth of 12 GHz. The resulting electrical signals are amplified with rf-amplifiers (AMP) and measured in the frequency

domain using an electrical spectrum analyzer (ESA) and in the time domain using an oscilloscope with 4 GHz analog bandwidth.

Special attention has been paid to achieve well defined coupling conditions. The optical pathlength between the SL is 51 mm resulting in a coupling time τ of 170 ps. To compare the intensity dynamics in the frequency domain with the time delay, we express the coupling time using the round trip frequency defined by $f_{RT} = 1/(2\tau) = 2.9$ GHz. The round trip frequency is in the same order of magnitude as the relaxation oscillation frequency. We are therefore in the regime of short coupling times. In order to estimate the coupling strength, we measure the photocurrent of one unpumped laser due to carrier excitation of the injected light from the respective other SL pumped at 60 mA. Under symmetrical coupling conditions the photocurrents are 118 ± 7 μA. We conclude that we obtain moderate coupling where a few percent of the output power of each SL is injected into its opponent.

A further issue to take care about is the effect of the feedback that the lasers get via reflections from the front facet of the opposing SL. To estimate this feedback strength, we measured the intensity of the reflected light. This results in an upper bound for the feedback strength of approximately 0.01%, which has been proven to be below the instability threshold of the lasers. We conclude that residual feedback may be present in the system, but that the coupling strength is at least 100 times larger compared to the feedback strength.

Another relevant parameter is the coupling phase. It is defined as $\Psi = \omega\tau$ where ω is the optical circular frequency of the uncoupled lasers without detuning. The coupling phase can be varied by two different methods. On the one hand, we can vary the coupling time τ by changing the coupling distance on a sub-wavelength scale. Alternatively, we can vary ω by shifting the temperature of both lasers simultaneously. The second method is the preferred one, as the coupling distance can be kept constant and the phase shift can be derived from the temperature shift. We note that we observed consistent experimental results with both methods.

3. INFLUENCE OF SPECTRAL DETUNING

To study the dynamical behavior of the coupled laser system depending on the spectral detuning Δf, we have chosen the following experimental procedure. The temperature of laser 2 is kept constant during the experiment. Laser 1 is detuned to a higher optical emission frequency with respect to laser 2. We define this direction of spectral detuning as positive. Now the temperature of laser 1 is increased in small steps resulting in a decreasing spectral detuning Δf. Since we change Δf between both lasers by detuning laser 1, laser 1 is denoted as *detuned laser* while laser 2 is kept under constant conditions and is therefore denoted as *stationary laser*. A total temperature variation of 4 K varies the spectral detuning between 24 and -24 GHz. After each step of changing Δf, the optical and the rf-spectra of the intensity dynamics are taken. We observe a characteristic evolution of the dynamical behavior depending on the spectral detuning which is illustrated in Fig. 2. For clarity, we call this evolution of the laser dynamics detuning scenario. The upper part (a) of Fig. 2 depicts the frequencies ν_{osc} of the intensity dynamics of both lasers. The filled circles mark frequencies whose intensity is more than 3 dB over the detection background extracted from the rf-spectra. As a reference, the continuous line indicates the nominal detuning of the uncoupled lasers. Fig. 2 (b) shows the emission wavelength of the two lasers taken from the peak position of the optical spectra. In addition to the wavelength scale, a shifted frequency scale is used where the spectral deviation from the free running laser frequency for zero detuning can be seen.

In Fig. 2 (b) we see that the stationary laser's frequency stays close to its free running frequency. The detuned laser shows a stair-like behavior of its optical frequency depending on the spectral detuning. We interpret the stair-like optical frequencies of the two lasers as the modes of the coupled laser system. In the following we denote them as coupled laser modes (CLM). Two different regimes can be distinguished in the detuning scenario. For small detuning we find a locking-region ranging from $\Delta f = 4.1$ GHz to $\Delta f = -7.0$ GHz where both lasers emit light at the same optical frequency and no intensity dynamics is measured in the rf-spectra. Within this locking-region we see three steps of the optical frequency in Fig. 2 (b) spanning detuning intervals of 7.7, 1.7 and 1.7 GHz, respectively. These three stairs correspond to three different stable CLM. Outside the locking-region we observe a continuation of the stair-like behavior of the CLM, but both lasers do not lock to the same optical frequency anymore. The stationary laser's frequency remains close to free running spectral position while the detuned laser exhibits transitions of its optical frequency depending on the detuning. In this regime the

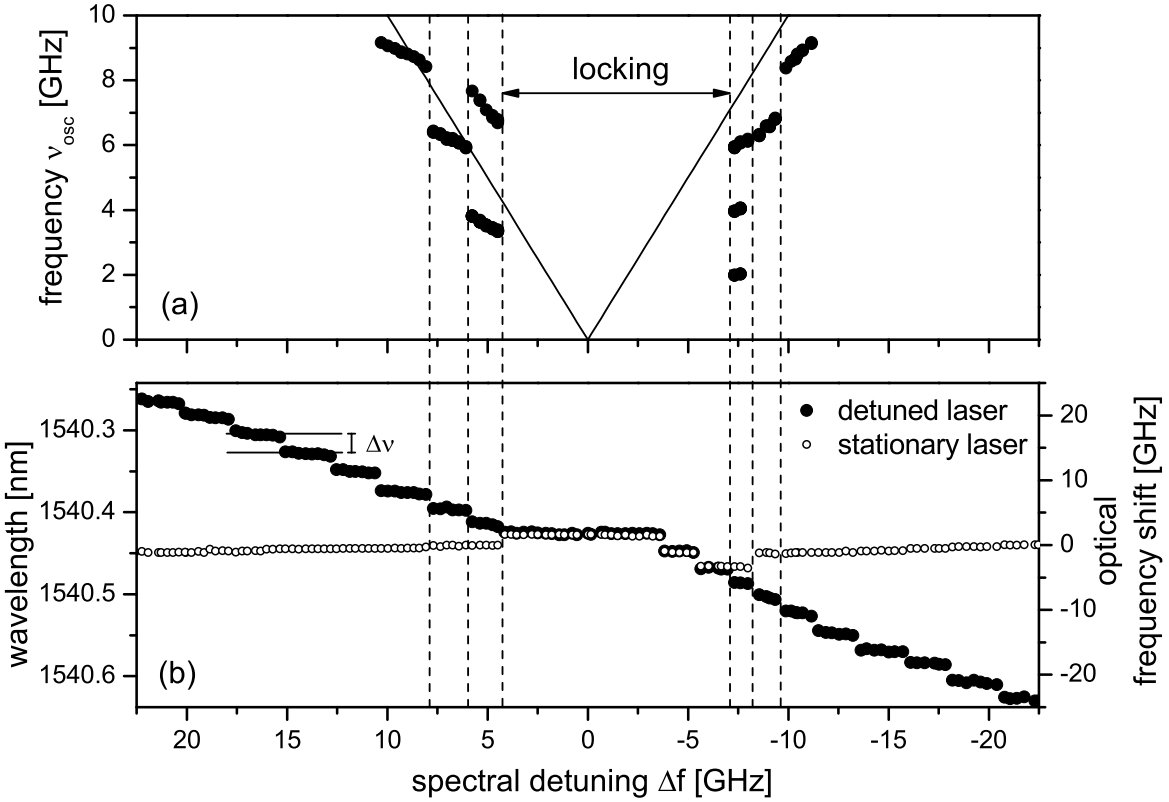

Figure 2. Experimental detunig scenario. Fig. (a) shows the frequencies ν_{osc} of the intensity dynamics depending on the spectral detuning Δf. The continuous line indicates the nominal detuning of the uncoupled lasers. Fig. (b) depicts the emission wavelength of the two lasers respectively their optical frequency shift relative to their free running frequency for zero detuning. Furthermore, an example of the optical frequency separation $\Delta\nu$ between two steps is shown.

intensity of both lasers exhibits periodic oscillations with frequencies ν_{osc} equal to the spectral deviation between the two optical frequencies. As a consequence, the frequency ν_{osc} of the intensity dynamics follows the stair-like behavior observed for the optical frequency shift outside the locking-region. These oscillation frequencies and their harmonics can be seen in Fig. 2 (a). We note that the range of frequencies presented is limited by our detection bandwidth. According to the stable CLM inside the locking-region we interpret the dynamic states outside the locking-region as unstable CLM. For spectral detunings larger than approximately ± 10 GHz the frequency steps of the detuned laser are very regular. Each unstable CLM spans a detuning interval of 2.4 ± 0.2 GHz. The separation of the optical frequencies of neighbored CLM is found to be $\Delta\nu = 2.8 \pm 0.4$ GHz. Close to and within the locking region the CLM are less regular. The average separation of two CLM is significantly smaller. In the locking region and in its proximity it lies around $\Delta\nu = 2$ GHz.

These experimental results demonstrate that the dynamical behavior of the delay-coupled system strongly depends on the coupling time. Beyond the locking-region, the oscillation frequencies of neighbored CLM are separated by $\Delta\nu = 2.8$ GHz, which is in good agreement with the round trip frequency of 2.9 GHz. Close to the locking-region the frequency separation of the CLM decreases. There are two physical reasons for $\Delta\nu$ being smaller than the round trip frequency $1/(2\tau)$. First, Dente et al. showed that the mode separation of two delay-coupled laser resonators is smaller than the round trip frequency of the system.[14] Second, $\Delta\nu$ is shifted to smaller values in dependence of the spectral detuning due to mutual frequency pulling. This second effect is similar to the well-known frequency pulling for SL with external optical injection.[15] Within the locking-region the coupled system emits on stable CLM, which are separated by less than the round trip frequency, too. The asymmetric structure of these modes with respect to the zero detuning point is a consequence of the α-parameter

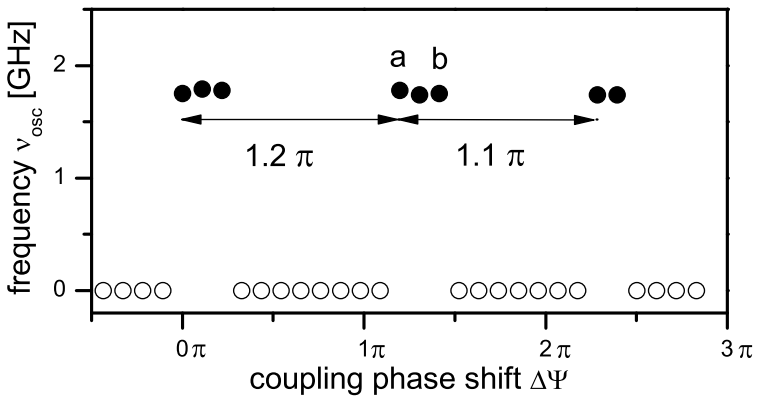

Figure 3. Fundamental frequency ν_{osc} of the intensity dynamics of the lasers in dependence on the coupling phase shift. Filled circles (•) show the fundamental frequency component of the dynamics. Hollow circles (○) indicate locking without intensity dynamics. The time series at the positions a and b are depicted in Fig. 4.

and the coupling phase. A detailed theoretical analysis of the mode structure of the locking region is presented elsewhere.[12,13] Therein, a bifurcation analysis of the rate equation model described in section 5 is performed. Here, we concentrate on the region of periodic oscillations outside the locking-region. In particular we concentrate on the transitions between the different CLM. We find that the coupling phase Ψ has a significant influence on the spectral detuning values at which these transitions occur. Therefore, the influence of the coupling phase will be discussed in the following section.

4. INFLUENCE OF THE COUPLING PHASE

In this section we study the influence of the coupling phase Ψ on the previously discussed detuning scenario. Therefore, we have performed experiments similar to the ones presented in the previous section, but instead of varying the temperature of only one laser, the temperatures of both lasers are varied simultaneously in small steps. Hence, the spectral detuning Δf between the lasers is kept constant, while the coupling phase Ψ changes. The step width $\Delta\Psi$ of the coupling phase is calculated from the temperature step ΔT of the lasers. Using the linear dependence of -12.1 GHz/K between the optical emission frequency and the temperature of the uncoupled lasers results in $\Delta\Psi = -4.1\pi\ \mathrm{K}^{-1}\Delta T$.

Fig. 3 depicts the fundamental frequency ν_{osc} of the intensity oscillations of the lasers in dependence on the coupling phase shift $\Delta\Psi$. Since the rf-spectra only contain information about the spectral intensity and not about the phase relation of the dynamics, we took simultaneous time series of the two intensities with the oscilloscope. The frequencies in Fig. 3 were obtained using Fourier transformation of the time series. The spectral detuning was $\Delta f = 5$ GHz being close to the border of the locking-region. Filled circles (•) show the fundamental frequency component of the dynamics, hollow circles (○) indicate locking without detectable intensity dynamics. A cyclic alternation between locking and periodic oscillation of $\nu_{osc} = 1.8$ GHz can be seen if the coupling phase is increased. The period is π within the accuracy of the coupling phase steps.

Two 5 ns intervals of two pairs of time series are shown in Fig. 4 (a) and (b). They correspond to the indicated points (a) and (b) in Fig. 3. The time series of the stationary laser are drawn with crosses (×) and interpolated with B-splines depicted in continuous lines, the time series of the detuned laser are drawn with circles (○) and interpolated with B-splines depicted in dashed lines. In both figures 4 (a) and (b) the phase relation $\delta\phi$ between the intensity oscillations of the two lasers is constant within one time series. But a comparison of figure (a) and figure (b) reveals a significant shift of the phase relation $\delta\phi$ between the intensity oscillations, since $\delta\phi$ increases from (a) to (b). This shift of the phase relation $\delta\phi$ occurs within the unstable CLM if the coupling phase Ψ is varied. While Fig. 4 shows results obtained for variation of the coupling phase Ψ by simultaneous temperature detuning of the lasers, the same shift of the phase relation $\delta\phi$ is measured if the coupling phase Ψ is changed by a variation of the coupling time τ.

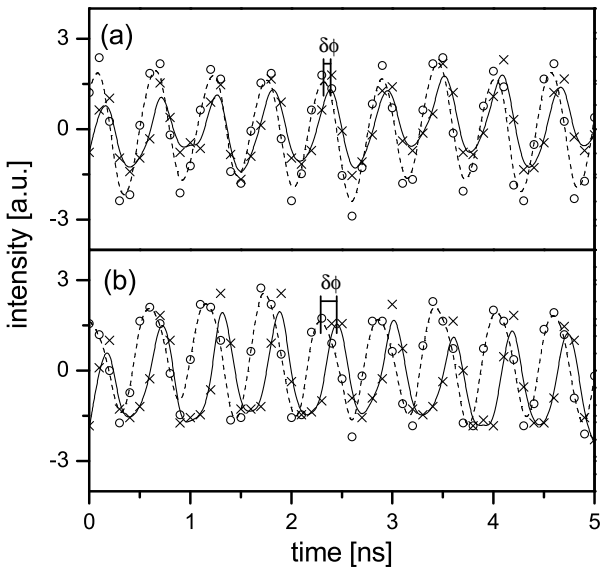

Figure 4. Intensity time series of the two lasers for different coupling phases. The time series of the stationary laser are drawn with crosses (×) and interpolated with B-splines depicted in continuous lines. The time series of the detuned laser are drawn with circles (○) and interpolated with B-splines depicted in dashed lines. Fig. (a) and (b) correspond to the positions (a) and (b) indicated in Fig. 3.

It becomes clear from these results, that transitions between the stable CLM and the unstable CLM do not only depend on the spectral detuning Δf but also on the coupling phase Ψ. Similar experimental results have been obtained for larger spectral detuning. In this case a π-cyclic scenario between two unstable CLM adjacent in the detuning scenario is measured if the coupling phase Ψ is varied as we will show in Fig. 6 for numerical results. Due to the limited bandwidth of the oscilloscope, the shift of the phase relation $\delta\phi$ between the two lasers can only be measured close to the locking-region where the oscillation frequency is significantly less than 4 GHz. The analysis of states with a higher oscillation frequency can be performed with the help of numerical simulations using a rate equation model.

5. MODELING

The numerical modeling presented in this section has three major reasons. First, studies of the symmetric situation of two identical lasers with well-defined model conditions can be performed. Second, we can analyze the dynamical behavior for larger spectral detuning beyond the bandwidth of our detection devices. Finally, in the model we can exclude unwanted external influences such as the residual feedback effects of the experiment.

The rate equations we use in our modeling are based on the well-known Lang-Kobayashi equations for SL with delayed optical feedback.[16] Instead of coupling the light back into the same laser, a symmetric cross coupling between two SL is realized. Recently, Mulet et al. have shown the equivalence of this phenomenological model with a more detailed model derived from Maxwell-Bloch equations in the limit where higher order terms in the coupling strength can be neglected.[17] This includes feedback effects as the feedback strength is proportional to the square of the coupling strength. The model equations for the two lasers are listed below:

$$\frac{dE_i(t)}{dt} = \tfrac{1}{2}\xi n_i(t)E_i(t) + \kappa E_{3-i}(t-\tau)\cos[\phi_{3-i}(t-\tau) - \phi_i(t) - \Psi] \quad (1)$$

$$\frac{d\phi_i(t)}{dt} = \tfrac{1}{2}\alpha\xi n_i(t) + \kappa\tfrac{E_{3-i}(t-\tau)}{E_i(t)}\sin[\phi_{3-i}(t-\tau) - \phi_i(t) - \Psi] + 2\pi\delta_{2,i}\Delta f \quad (2)$$

$$\frac{dn_i(t)}{dt} = (j-1)\gamma_e N_{Schw} - \gamma_e n_i(t) - [\gamma_p + \xi n_i(t)]E_i(t)^2 \quad (3)$$

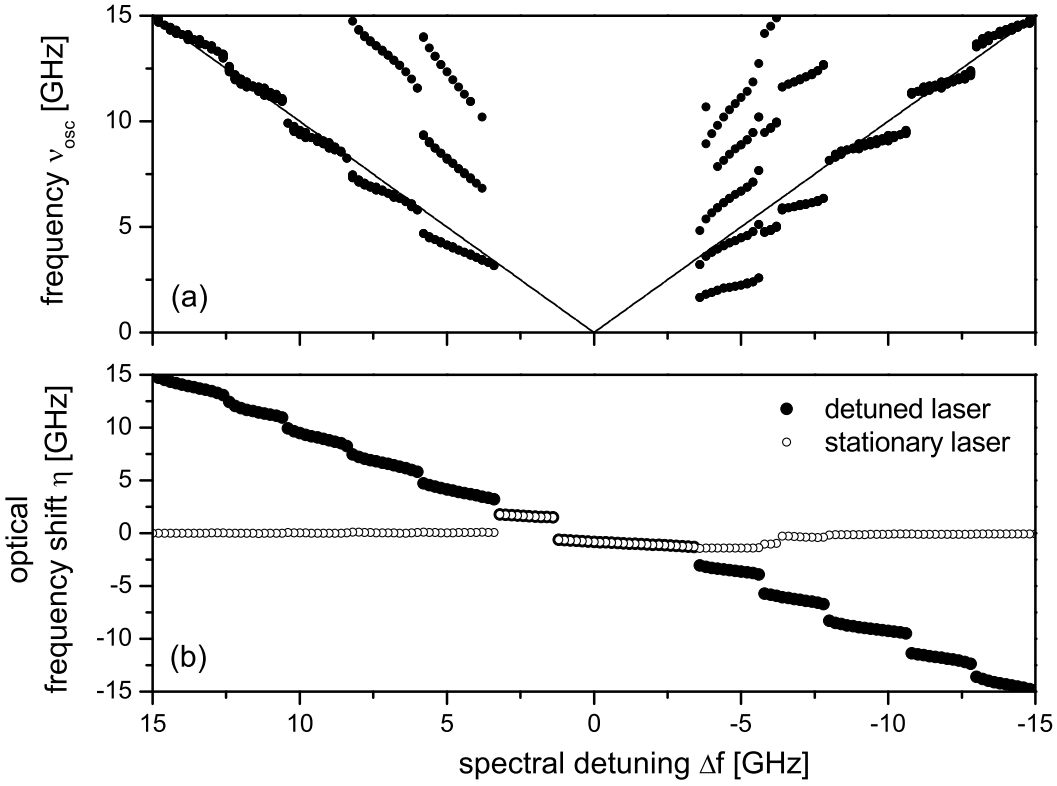

Figure 5. Modeled detuning scenario. The frequencies ν_{osc} of the intensity dynamics depending on the spectral detuning are shown in Fig. (a). The continuous line indicates the nominal detuning of the uncoupled lasers. Fig. (b) depicts the optical frequency shift η of the two lasers relative to their free running frequency for zero detuning.

α	2		α-parameter
ξ	$0.8 \cdot 10^{-15}$	$\mathrm{cm}^3/\mathrm{ns}$	differential gain
κ	7	ns^{-1}	coupling rate
τ	0.17	ns	coupling time
j	7		injection current (normalized to the threshold current)
γ_e	1	ns^{-1}	carrier decay rate
N_{Schw}	10^{18}	cm^{-3}	carrier density at the threshold current
γ_p	150	ns^{-1}	photon decay rate
Ψ	$0 \ldots 2\pi$		coupling phase
Δf	$-15 \ldots 15$	GHz	spectral detuning

Table 1. Parameters of the model equations (1) to (3)

The time dependent variables of the equations are the photon density E^2, the phase ϕ and the excess carrier density n. The index $i \in \{1, 2\}$ indicates the two lasers. The parameters are listed in Tab. 1. We numerically integrate the six equations (1) to (3) and obtain time series of the intensity dynamics. The frequencies of the dynamics are taken from the Fourier transformation of the photon density. The optical frequency shift is defined by $\eta_i = \langle(\phi_i(t) - \phi_i(t-\tau))/\tau\rangle$, where $\langle\cdot\rangle$ stands for the temporal mean.

To compare the model with the experimental results we analyze the dynamical behavior of the model in dependence of the spectral detuning Δf with a fixed coupling phase Ψ. The results are presented in Fig. 5 in the same form of representation as the experimental results in Fig. 2. Comparing both figures, we find

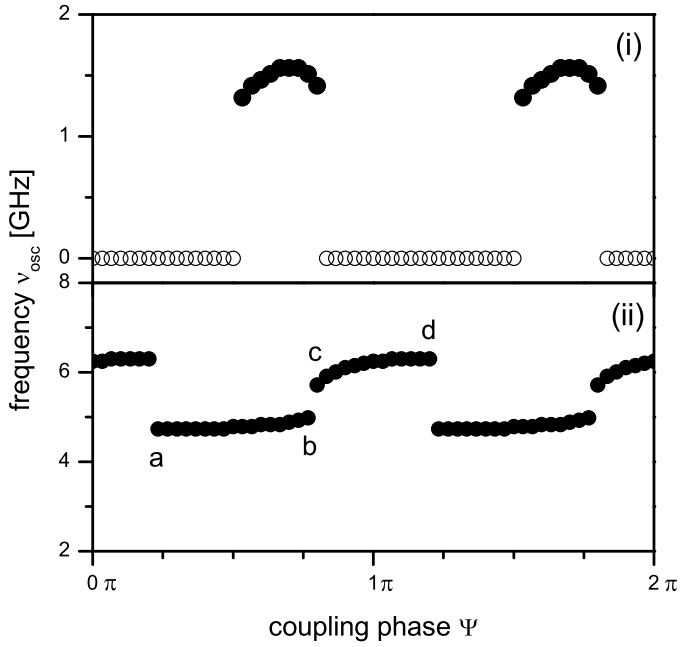

Figure 6. Fundamental frequency ν_{osc} of the modeled intensity dynamics of the lasers in dependence of the coupling phase. Filled circles (•) show the fundamental frequency component of the dynamics, hollow circles indicate locking with stable emission. The spectral detuning is $\Delta f = 3$ GHz in Fig. (i) and $\Delta f = 6.5$ GHz in Fig. (ii). The time series at the positions (a) to (d) are depicted in Fig. 7.

excellent agreement. Indeed, the model equations reveal the same detuning scenario as presented and discussed in section 3. We emphasize that the rate equation model does not include feedback effects. This nicely confirms that the instabilities are indeed induced by the delayed coupling.

The excellent agreement of the experimental and modeled detuning scenario allows to use the model to gain further insights into the dynamical behavior for larger spectral detuning. Therefore, we performed model calculations analogous to the experiments presented in section 4 in order to study the role of the phase difference $\Delta\phi$ of the oscillations of both lasers. Fig. 6 depicts two π-cyclic scenarios in which the dynamics of the coupled lasers alternate between two CLM. As for the experimental results in Fig. 3, the fundamental frequency ν_{osc} of the intensity dynamics is shown with filled circles (•) for different coupling phases ranging from $\Psi = 0$ to $\Psi = 2\pi$. Hollow circles (○) again represent locking without dynamics. The results in Fig. 6 (i) were calculated for a spectral detuning of $\Delta f = 3.0$ GHz which is close to the border of the locking-region in the modeled detuning scenario. The dynamics change in π-periodic cycles of the coupling phase between the stable CLM and the unstable CLM with a fundamental frequency of about $\nu_{osc} = 1.5$ GHz. Again we see excellent agreement between experimental and modeled results and proceed with higher spectral detuning. In Fig. 6 (ii) the spectral detuning has been chosen to be $\Delta f = 6.5$ GHz. Here, the dynamics change in π-periodic cycles between two unstable CLM with fundamental intensity oscillation frequencies of about $\nu_{osc} = 4.8$ GHz and about $\nu_{osc} = 6.2$ GHz. The experimental laser system shows the same cycles. But these CLM could not be analyzed experimentally in the time domain as the oscillation frequencies are beyond the 4 GHz bandwidth of the oscilloscope.

The modeled time series of the intensity dynamics for the positions (a) to (d) in Fig. 6 (ii) are represented in Fig. 7. The time series of the stationary laser are drawn with continuous lines, whereas the time series of the detuned laser are drawn with dashed lines. The time series show that in all cases the dynamics of the two lasers are nonidentical. Nevertheless, from the Fourier transformation of the time series we know that the frequencies are always identical for both lasers and only the power of the frequency components are different for the two lasers. In addition to this asymmetric behavior, the time series show a shift of the phase difference $\Delta\phi$ between the intensity oscillations if the optical coupling phase Ψ is varied. Interestingly, in Fig. 7 (a) the intensity oscillations

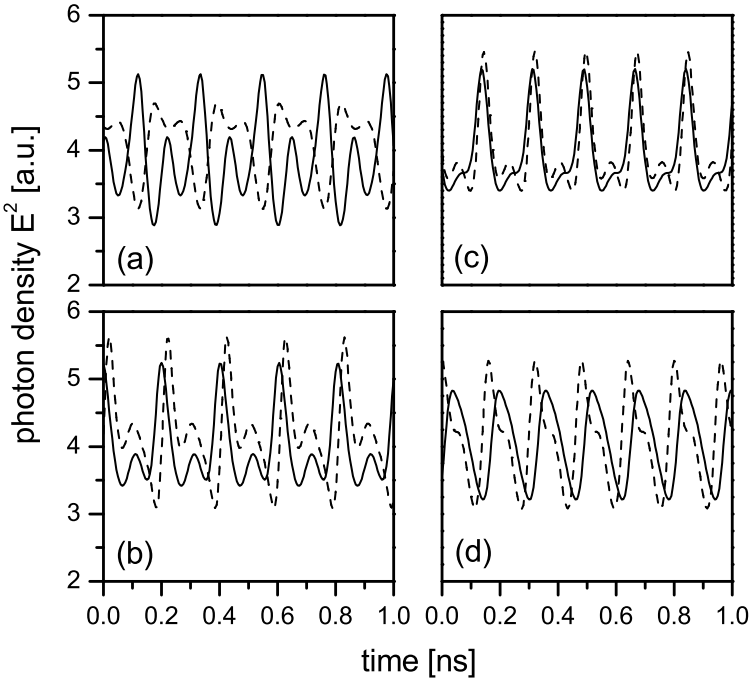

Figure 7. Modeled time series of the two lasers for different coupling phases. The time series of the stationary laser are represented in continuous lines, the time series of the detuned laser in dashed lines. Fig. (a) to (d) correspond to the positions indicated in Fig. 6 (ii).

of both lasers are anticorrelated. For increasing the coupling phase about $\pi/2$ the oscillations are correlated as it can be seen in Fig. 7 (b). In the case of the CLM with the larger fundamental frequency at $\nu_{osc} = 6.2$ GHz the time series in Fig. 7 (c) and (d) also show a shift of the phase relation. In agreement with the experimental observations our results give evidence that the phase difference $\Delta\phi$ between the laser oscillations depends on the coupling phase Ψ even for larger spectral detunings values.

6. CONCLUSIONS

In this work we have analyzed the intensity dynamics of device-identical delay-coupled SL for short coupling times and moderate coupling strength. We find stable and unstable coupled laser modes (CLM). The stable CLM exist for small spectral detuning Δf where both lasers lock to the same optical frequency and no intensity dynamic is present. Outside the locking-region, where both lasers emit at different optical frequencies, unstable CLM exist. In this regime we find periodic intensity oscillations with a fundamental frequency ν_{osc} equal to the spectral separation between the two lasers. Our results show that the spectral positions of different CLM are separated by a frequency related to the inverse of twice the coupling time. Therefore, a variation of the spectral detuning Δf or of the coupling phase Ψ induces mode jumps of the coupled laser system. From these results we conclude, that the delay, the spectral detuning and the coupling phase have an important influence on the structure of the CLM and therefore on the dynamics of the coupled lasers. We presented results obtained from numerical modeling based on rate equations showing excellent agreement with the experimental observations. The modeled results confirm that the observed structure of the CLM are an effect of the coupling delay. The influence of residual feedback of the experimental setup can be neglected.

In addition to these results we presented analysis of time series of the intensity dynamics. From the calculated time series we learn that the two lasers lock to the same oscillation frequencies, but have different amplitudes of the frequency components. Furthermore, the phase relation $\Delta\phi$ between the oscillations of both lasers has been found to be dependent on the coupling phase Ψ.

In summary, these results characterize the global dynamical behavior of the delay-coupled laser system over a wide parameter range. Together with a theoretical analysis of the bifurcation properties[12,13] we have achieved a good understanding of the detuning scenario.

ACKNOWLEDGMENTS

We thank Dr. Kenton White of Nortel Networks for providing us with the excellent semiconductor laser structures.

REFERENCES

1. H. Haken, "Effect of delay on phase locking in a pulse coupled neural network," *Eur. Phys. J.* **B 18**, pp. 545–550, 2000.
2. J. Weiner, R. Holz, F. W. Schneider, and K. Bar-Eli, "Mutually coupled oscillators with time delay," *J. Phys. Chem.* **96**, pp. 8915–8919, 1992.
3. D. V. R. Reddy, A. Sen, and G. L. Johnston, "Experimental evidence of time-delay-induced death in coupled limit-cycle oscillators," *Phys. Rev. Lett.* **85**, pp. 3381–3384, 2000.
4. S. H. Strogatz, "Death by delay," *Nature* **394**, pp. 316–317, 1998.
5. J. Mulet, C. Mirasso, T. Heil, and I. Fischer, "Synchronization scenario of two distant mutually coupled semiconductor lasers," *J. Opt. B: Quantum Semiclass. Opt.* **6**, pp. 97–105, 2004.
6. I. Fischer, Y. Liu, and P. Davis, "Synchronization of chaotic semiconductor laser dynamics on subnanosecond time scales and its potential for chaos communication," *Phys. Rev.* **A 62**, p. 011801, 2000.
7. "Feature section on optical chaos and applications to cryptography," *IEEE J. Quantum Electron.* **QE-38**, 2002.
8. M. Möhrle, B. Sartorius, C. Bornholdt, S. Bauer, O. Brox, A. Sigmund, R. Steingrüber, M. Radziunas, and H.-J. Wünsche, "Detuned grating multisection-RW-DFB lasers for high speed optical signal processing," *IEEE J. Select. Topics Quantum Electron.* **7**, pp. 217–223, 2001.
9. T. Heil, I. Fischer, W. Elsäßer, J. Mulet, and C. R. Mirasso, "Chaos synchronization and spontaneous symmetry-breaking in symmetrically delay-coupled semiconductor lasers," *Phys. Rev. Lett.* **86**, pp. 795–798, 2001.
10. J. Javaloyes, P. Mandel, and D. Pieroux, "Dynamical properties of lasers coupled face to face," *Phys. Rev.* **E 67**, p. 036201, 2003.
11. J. K. White, M. Matus, and J. V. Moloney, "Achronal generalized synchronization in mutually coupled semiconductor lasers," *Phys. Rev. E* **65**, p. 036229, 2002.
12. H. Erzgräber, D. Lenstra, B. Krauskopf, and I. Fischer, "Dynamical properties of mutually delayed coupled semiconductor lasers," *Proc. SPIE Photonics Europe 2004* , 2004.
13. E. Wille, *Nichtlineare Dynamik von zeitverzögert gekoppelten Halbleiterlasern im Bereich kurzer Kopplungszeiten*. diploma thesis, Technische Universität Darmstadt, Darmstadt, 2004.
14. G. C. Dente, C. E. Moeller, and P. S. Durkin, "Coupled oscillators at a distance: Applications to coupled semiconductor lasers," *IEEE J. Quantum Electron.* **QE-26**, pp. 1014–1022, 1990.
15. G. H. M. van Tartwijk, *Semiconductor Laser Dynamics with Optical Injection and Feedback*. Dissertation, Vrije Universiteit te Amsterdam, Amsterdam, 1994.
16. R. Lang and K. Kobayashi, "External optical feedback effects on semiconductor injection laser properties," *IEEE J. Quantum Electron.* **QE-16**, pp. 347–355, 1980.
17. J. Mulet, C. Masoller, and C. R. Mirasso, "Modeling bidirectionally coupled single-mode semiconductor lasers," *Phys. Rev.* **A 65**, p. 063815, 2002.